

# NASA Contractor Report 177991

(NASA-CR-177991) MIXED-MODE CYCLIC  
DEBONDING OF ADHESIVELY BONDED COMPOSITE  
JOINTS M.S. Thesis (Missouri Univ.) 59 p  
HC A04/MP A01

N86-12255

CSEL 11D

G3/24

Unclass  
04770

MIXED-MODE CYCLIC DEBONDING OF  
ADHESIVELY BONDED COMPOSITE JOINTS

Mohammad Ali Rezaizadeh  
and Shankar Mall

UNIVERSITY OF MISSOURI  
Rolla, Missouri

Grant NAG1-425  
October 1985

**NASA**

National Aeronautics and  
Space Administration

Langley Research Center  
Hampton, Virginia 23665



## ABSTRACT

A combined experimental-analytical investigation to characterize the cyclic failure mechanism of a simple composite-to-composite bonded joint was conducted. The cracked lap shear (CLS) specimens of graphite/epoxy adherend bonded with EC-3445 adhesive were tested under combined mode I and II loading. In all specimens tested, fatigue failure occurred in the form of cyclic debonding. The cyclic debond growth rates were measured. The finite element analysis was employed to compute the mode I, mode II, and total strain energy release rates (i.e.  $G_I$ ,  $G_{II}$ , and  $G_T$ ). A wide range of mixed-mode loading, i.e.  $G_I/G_{II}$  ranging from 0.03 to 0.38, was obtained. The total strain energy release rate,  $G_T$ , appeared to be the driving parameter for cyclic debonding in the tested composite bonded system.

## ACKNOWLEDGEMENT

The author wishes to express his sincere gratitude to his advisor, Dr. S. Mall, for his constant guidance and support throughout this research and the course of study at the University of Missouri-Rolla. The author also thanks Dr. L.R. Dharani, Dr. A.G. Haddock and Dr. M.M. Tang for serving as committee members and reviewing this thesis. Thanks are extended to Dr. W.S. Johnson, NASA Langley Research Center for supplying test specimens used in the research. The partial financial support of the NASA Langley Research Center is also gratefully acknowledged.

The author also wishes to extend thanks to chairman, Dr. P.G. Hansen, and staff of the Department of Engineering Mechanics for providing a teaching assistantship during the course of study at the University of Missouri-Rolla.

Finally, the author wishes to express his sincere thanks to his family for their continued support and encouragement during his study.

## TABLE OF CONTENTS

	PAGE
ABSTRACT.....	1
ACKNOWLEDGEMENT.....	iii
LIST OF FIGURES.....	vii
LIST OF TABLES.....	ix
I. INTRODUCTION.....	1
II. LITERATURE REVIEW.....	4
III. EXPERIMENTS.....	10
A. SPECIMEN PREPARATION AND CONFIGURATION.....	10
B. TESTING SYSTEM.....	12
C. TESTING PROCEDURE.....	15
D. TEST RESULTS.....	15
1. Debond Measurment.....	15
2. Debond Surfaces.....	18
IV. FINITE ELEMENT ANALYSIS.....	21
A. BGUNDARY CONDITION.....	23
B. DEBOND LOCATION.....	26
C. LOAD LEVEL.....	28
D. DEBOND LENGTH.....	28
V. RESULTS AND DISCUSSIONS.....	33
A. THE INTERACTION OF MIXED-MODE LOADING ON CYCLIC DEBONDING.....	33
B. THE EFFECT OF STRESS RATIO ON CYCLIC DEBONDING.....	42

PRECEDING PAGE BLANK NOT FILMED

TABLE OF CONTENTS (Cont.)	PAGE
VI. CONCLUSIONS.....	45
BIBLIOGRAPHY.....	47

## LIST OF FIGURES

FIGURES	PAGE
1. Cracked Lap Shear Specimen.....	11
2. Fatigue Testing Machine.....	14
3. Linear Variation of Debond Growth with Fatigue Cycle for a Thin Strap (32/16) Specimen at 131 MPa Stress.....	16
4. Nonlinear Variation of Debond Growth with Fatigue Cycle for a Thin Strap (32/16) Specimen at 140 MPa Stress.....	17
5. Typical Debond Growth Data at Different Stress Levels for a Thin Strap (32/16) Specimen.....	19
6. Debonded Surfaces of Cracked Lap Shear Specimen with 32 Ply Strap and 16 Ply Lap.....	20
7. Finite Element Model.....	22
8. Lateral Deflection of a Thick Strap (16/32) Specimen with a Crack Length of 50.8 mm at 82 MPa Stress.....	24
9. Variation of Strain Energy Release Rate with Location of Debond within Adhesive for Thick Strap (16/32) Specimen at 82 MPa Stress.....	27
10. Variation of Strain Energy Release Rates with Applied Stress for Thick Strap (16/32) Specimen with a Crack Length of 50.8 mm .....	29

LIST OF FIGURES (Cont.)	PAGE
11. Variation of Strain Energy Release Rates with Debond Length for Thick and Thin Strap Specimens..	31
12. Comparison of Relationship Between $G_I$ Versus Debond Growth Rate.....	34
13. Comparison of Relationship Between $G_{II}$ Versus Debond Growth Rate.....	35
14. Comparison of Relationship Between $G_T$ Versus Debond Growth Rate.....	36
15. Relation Between $G_I$ and Debond Growth Rate.....	38
16. Relation Between $G_{II}$ and Debond Growth Rate.....	39
17. Relation Between $G_T$ and Debond Growth Rate.....	40
18. Effect of Stress Ratio on the Relation Between Total Strain Energy Release Rate and Debond Growth Rate.....	43
19. Effect of Stress Ratio on the Relation Between Total Strain Energy Release Rate Range and Debond Growth Rate.....	44

## LIST OF TABLES

	PAGE
TABLE I. Adhesive Material Properties.....	13
TABLE II. Graphite/Epoxy Adherend Material Properties.....	13
TABLE III. Effect of Lateral Deflection on G Calculation of Thick Strap (16/32) Specimen with Crack Length of 50.8 mm at 82 MPa Stress.....	25
TABLE IV. Variation of Strain Energy Release Rate with Applied Stress for Thick Strap (16/32) Specimen with Crack Length of 50.8 mm.....	30



## I. INTRODUCTION

The word "Composite" in the expression composite material signifies that two or more constituents are combined on a macroscopic scale to form a new and useful material. Composite materials have a long history of usage. Currently, many aerospace and other industries are developing products made with fiber reinforced composite materials. These materials offer excellent strength-to-weight and stiffness-to-weight ratios.

The efficient utilization of reinforced composite materials requires development of better methods of joining structural components than used in metallic structures. Because composites are severely weakened by mechanical fastener holes, adhesive bonding is a desirable alternative to mechanical fastening. Adhesive bonding offers several advantages: lower structural weight; less expensive fabrication techniques; and no strength degradation of basic laminate due to fastener holes.

Design methods for adhesively bonded composites require criteria to predict both strength and durability. Although, a great deal of analytical and experimental works have been reported on the static strength of bonded composites (e.g. see Ref. 1,2), very little information is available on their fatigue behavior. Several possible fatigue failure modes

exist for bonded composites: cyclic debonding (i.e. progressive separation of the adhesive bond under cyclic load), cyclic delamination (i.e. interlaminar damage), adherend fatigue, or a combination of these. Therefore, the reliable life predictions of composite bonded joints under fatigue loading require the complete understanding of the mechanics associated with each failure mode. This study will, however, focus only on one of these failure modes, i.e. the mechanics of cyclic debonding.

Many of the results obtained in cyclic debonding studies of composite-to-metal joints<sup>(3)</sup> and metal-to-metal joints<sup>(4,5)</sup> may be applicable to the study of composite-to-composite joints. Previous researchers<sup>(3-5)</sup> have shown that the strain energy release rate defined from fracture mechanics principles can be used to correlate the cyclic debonding rate. This is similar to the approach in metals where fatigue crack propagation rate is correlated with the strain energy release rate. Cyclic debonding of adhesively bonded composite joints was investigated with the cracked lap shear (CLS) specimen by Mall et al.<sup>(6)</sup> Two different geometries of CLS specimen were tested under cyclic loading with stress ratio of 0.1. Data from these two specimens were used to determine the fracture mode dependence of cyclic debonding. The cyclic debond growth rate correlated better with the total strain energy release rate,  $G_T$ , than it did with either  $G_I$  or  $G_{II}$  independently.

The previous study by Mall et al.<sup>(6)</sup> was, later on, extended to investigate cyclic debonding under opening mode load with double cantilever beam (DCB) specimen.<sup>(7)</sup> The relations  $G_I$  versus  $da/dN$  from the DCB specimens and  $G_T$  versus  $da/dN$  from the CLS specimens agreed with each other, where  $G_I$  is total (and also opening mode I) strain energy release rate for DCB specimens, and  $G_T$  is total strain energy release rate for CLS specimen. The relation  $G_I$  versus  $da/dN$  from the CLS specimen under mixed-mode loading did not, however, agree with the relation  $G_I$  versus  $da/dN$  from the DCB specimen under the opening mode I loading. The results of this study<sup>(7)</sup>, thus, suggested that the cyclic debond failure in the adhesively bonded composite joints is governed by total strain energy release rate.

Since the previous study<sup>(6)</sup> used two geometries of CLS specimen which provided a rather narrow range of mixed-mode loading (i.e.  $G_I/G_{II}$  ranged from 0.25 to 0.33), further study was considered appropriate to investigate the cyclic debonding for wide range of mixed-mode loading. For this purpose, two new geometries of cracked lap shear specimen were tested, which provided  $G_I/G_{II}$  ranging from 0.03 to 0.38. In addition, the effect of stress ratio on cyclic debonding were undertaken in this study. The details and results of these investigation are presented in the successive chapters.

## II. LITERATURE REVIEW

Adhesive joints usually fail by the initiation and propagation of flaws and, since the basic principle of fracture mechanics theories is that the strength of materials is governed by the presence of flaws, the application of such theories to adhesive joint failure has received considerable attention.<sup>(8)</sup> Great deal of work on the static strength of bonded joints based on fracture mechanics principle has been reported (e.g. see References 1,2), however, very little information is available on their durability and fatigue behavior.

The first study in the fatigue behavior of composite-to-metal joints was reported in 1976 by Roderick et al.<sup>(9)</sup> They used fracture mechanics concept of strain energy release rate to model the cyclic failure of bonded joints. For this purpose, two types of specimens made of graphite/epoxy bonded to aluminum and S-glass/epoxy bonded to aluminum were tested under constant amplitude cyclic loading. Both room temperature and elevated temperature curing adhesives were used. They showed that the debonding rates were influenced by both adherend thickness and the stress ratio. For a given maximum stress, a lower stress ratio and a thicker specimen produced faster debonding. The different forms of strain energy release rate correlated the different material systems, but empirical correlating expressions applicable to

one bonded system were not appropriate for another bonded system. Therefore, a definite correlation between strain energy release rate and debond growth rate could not be determined.

In 1978, Brussat and Chiu<sup>(10)</sup> analyzed metal-to-metal joints under constant amplitude cyclic loading. The authors investigated the crack propagation in the adhesive layer under cyclic loading in laboratory ambient conditions. For this purpose, they tested cracked lap shear and width tapered beam specimens of 7075-T6 aluminum adherends bonded to AF-55S adhesive with initial bondline flaws at stress ratio of 0.1 and a cyclic frequency of 3 Hz. A comparison of pure mode I and mixed-mode data indicated that the  $G_I$  has a significant effect on crack growth rates. Analytical crack growth estimates were obtained from these tests using a linear elastic fracture mechanics (LEFM) approach for real structural joints. This approach led to a reasonably good crack growth predictions of several tested joints.

The investigation of fatigue failure of the environmentally-conditioned (i.e. different temperature and humidity conditions) metal-to-metal joint was conducted by Romanko et al.<sup>(11)</sup> They studied the two joint models (i.e. cracked lap shear and thick adherend specimens) to characterize the time dependent fracture in adhesive bonded joints. Although this study<sup>(11)</sup> lacked in any definite conclusion about cyclic debonding, however several test data

with FM-73 adhesive were generated in this program. This program was later on continued at Chemical Systems Division of United Technologies. (12)

Recently, cyclic debonding of metal-to-metal joint under mixed-mode loading was conducted by Everett and Johnson. (13)

They employed an experimental investigation to assess the repeatability of debond growth rates. This was done by using two sets of cracked lap shear specimens consisting of aluminum 7075-T6 adherends bonded with FM-73 adhesive. These specimens were same as those used in previous studies by Romanko et al. (11) and Francis et al. (12) The test results indicated that debond growth rates from both specimens were within the scatter band which is similar to that observed in fatigue crack growth in metals. Cyclic debonding occurred at strain energy release rates that were more than an order of magnitude less than the critical strain energy release rate in static test.

Jablonski (14) performed the fatigue test on metal-to-metal joints consisting of aluminum alloy 2024-T35 as the adherend and two high temperature structural adhesives, AF-163 and EA-9649. He employed the tapered double cantilever beam specimen to investigate the cyclic debonding. The crack closure load developed as a result of fatigue crack propagation. The test results showed that there was a higher correlation between fatigue crack growth rate and effective strain energy release rate than between fatigue crack growth

rate and strain energy release range. Also, the fatigue failure always followed a cohesive fracture path.

The first analytical and experimental study of fatigue failure of composite-to-composite joint was conducted by Renton and Vinson.<sup>(15)</sup> They examined the influence of certain geometric variations of the lap joint configuration, such as overlap length and the orientation of the laminae of the laminated adherends, on the fatigue life of the joint. Their test results indicated that the proportional limit has a significant influence on the fatigue life of a bonded joint, that up to a 40-percent load penalty occurred for an angle ply construction versus an all  $0^\circ$  layup and that the absolute magnitude of load withstood by the joint for a given number of cycles increased with overlap length.

Using composite-to-metal joints, Everett<sup>(16)</sup> employed a combined experimental and analytical study to determine the role of peel stresses on cyclic debonding. Experimentally, he created the compressive normal stress by applying a clamping force to oppose the peel stress in the bondline. The effect of different values of clamping force on the cyclic debond was tested to determine the clamping force that was just sufficient to stop or to decrease the debond growth rate. He conducted the finite element analysis to assess the effect of the clamping force on the strain energy release rates due to shear and peel stresses.

In 1982, Dattaguru et al. (17) performed a finite element analysis of cohesive failure on cracked lap shear specimen. A two dimensional finite element analysis was used. The analysis accounted for the geometric non-linearity associated with large rotations in unsymmetric joints. Results showed that non-linear effects due to large rotations, significantly affect the calculated mode I and II strain energy release rates. The ratio of mode I to mode II strain energy release rates was also found to be strongly affected by the adhesive modulus and the adherend thickness.

In a recent study, cyclic debonding of composite-to-composite joints was investigated by Mall, Johnson, and Everett. (6) This study focused on the correlation of the measured cyclic debonding rates with strain energy release rates using finite element method. Also, the influence of mode I and II was investigated on debond rate. Two bonded systems were studied, i.e. graphite/epoxy adherends bonded with EC-3445 and FM-300 adhesives. For each bonded system, two types of specimen were tested: 1) lap adherend of 8 plies bonded to a strap adherend of 16 plies, and 2) lap adherend of 16 plies bonded to a strap adherend of 8 plies. The results showed that  $G_I/G_{II}$  for all specimens were all within the narrow range of 0.25 to 0.38. Therefore,  $G_I$ ,  $G_{II}$ , and  $G_T$  correlated reasonably good with debond growth rate. But the total strain energy release rate,  $G_T$ , showed a better correlation than either  $G_I$  or  $G_{II}$ . Also, the debond always grew in the region of the



adhesive that had the highest mode I loading. This indicated that  $G_I$  had a stronger influence than  $G_{II}$  on debond location. This study was later carried on to investigate the cyclic debonding under opening mode I load with composite double cantilever beam (DCB) specimen.<sup>(7)</sup> The results of this study, further, suggested that the  $G_I$  is the driving parameter for cyclic debonding in composite bonded joints. Johnson and Mall<sup>(18)</sup> have also shown that total strain energy release rate was the parameter which governed the initiation of cyclic debonding, and hence they have suggested a design procedure for composite bonded joints based on fracture mechanics principle.

### III. EXPERIMENTS

#### A. SPECIMEN PREPARATION AND CONFIGURATION

The cracked lap shear (CLS) specimen, shown in Figure 1, was employed for this study because it represents a joint subjected to in-plane mixed-mode loading and large area bonds typical of many structural applications. The different thicknesses of strap and lap adherends are intended to provide a different mixture of mode I and mode II strain energy release rates.<sup>(17)</sup> In the present study, the cracked lap shear specimen had the strap and lap adherends of 16 or 32 plies. This arrangement provided two types of specimen: 1) thin lap adherend of 16 plies bonded to a thick strap adherend of 32 plies (16/32); and 2) thick lap adherend of 32 plies bonded to a thin strap adherend of 16 plies (32/16). The length of strap and lap adherends were 381 and 254 mm, respectively. However, a total of 127 mm was needed for grip support on both ends. These specimens had no initial crack.

The bonded system consists of graphite/epoxy (T300/5208) adherends bonded with EC-3445 adhesive. The EC-3445 adhesive is a thermosetting paste adhesive with a cure temperature of 121°C. Specimen fabrication was performed by the conventional secondary bonding procedure. The bonding process followed the manufacturers' recommended procedure and was done at NASA Langley Research Center. The nominal adhesive thickness was 0.10 mm. The Young's modulus of EC-3445 was calculated from

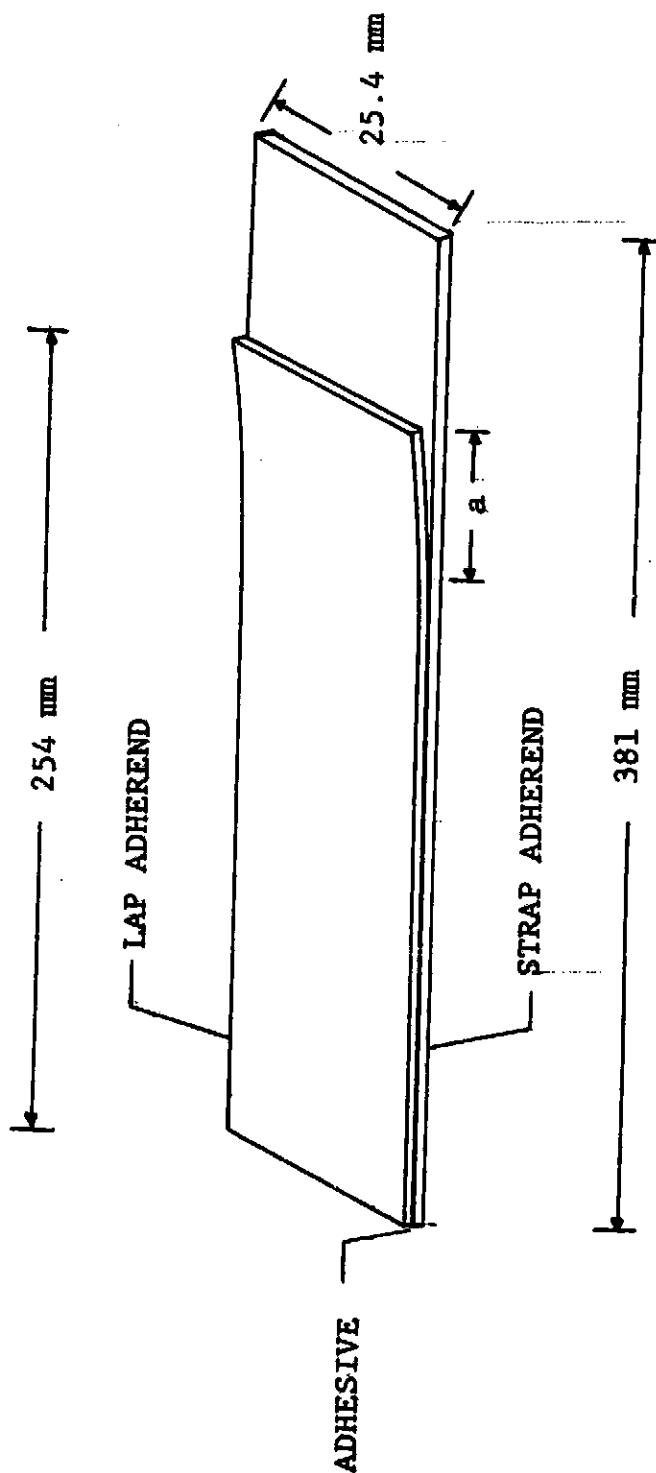


Figure 1. Cracked Lap Shear Specimen

the shear modulus of AF-55 adhesive film, because the EC-3445 adhesive is the paste version of the AF-55.<sup>(12)</sup> The EC-3445 adhesive was assumed an isotropic material. The material properties of EC-3445 adhesive are presented in Table I.

The cracked lap shear specimen consisted of lap and strap adherends with quasi-isotropic layups of  $(0^\circ/45^\circ/-45^\circ/90^\circ)_{2S}$  and  $(0^\circ/45^\circ/-45^\circ/90^\circ)_{4S}$ . The adherends were bonded to the adhesive with  $0^\circ$  ply at interface with adhesive. Material properties of graphite/epoxy are given in Table II.

#### B. TESTING SYSTEM

All fatigue test results presented and discussed in this paper were obtained through the use of a MTS closed loop servo-hydraulic testing system. The illustration in Figure 2 shows the load frame (right) and controller console (left). Although not fully exploited in this study, the system permits great versatility through the inherent advantage of being able to conduct complex testing sequences.

The load frame is capable of axial loading to  $\pm 20,000$  lb ( $\pm 88.9$  KN). Load is measured by an axial load cell, Model no. 1020 JL. All testing during this program was conducted under load controlled condition, wherein the load desired was input via the controller. This machine can be operated by a function generator capable of producing waveforms such as sinusoidal, triangular, and square signals.

TABLE I  
ADHESIVE MATERIAL PROPERTIES

	Modulus		Poisson's Ratio
	E (GPa)	G	$\nu$
EC-3445 (3M Company)	1.81	0.65	0.4

TABLE II  
GRAPHITE/EPOXY<sup>a</sup> ADHEREND MATERIAL PROPERTIES

Modulus <sup>b</sup>			Poisson's Ratio <sup>b</sup>	
E <sub>1</sub>	E <sub>2</sub> (GPa)	G <sub>12</sub>	$\nu_{12}$	$\nu_{21}$
131.0	13.0	6.4	.34	0.35

<sup>a</sup>T300/5208 (NARMG0), fiber volume fraction is 0.63.

<sup>b</sup>The subscript 1,2, and 3 correspond to the longitudinal, transverse, and thickness directions, respectively, of a unidirectional ply.

ORIGINAL PAGE IS  
OF POOR QUALITY



Figure 2. Fatigue Testing Machine

### C. TESTING PROCEDURE

The objective of the test program was to measure the debond growth rate under fatigue loading. For this purpose, the uniaxial fatigue tests were run using a frequency of 10 Hz sine wave. All fatigue test specimens were tested under constant amplitude cyclic loads. The R-ratios (ratio of minimum to maximum stress) used in the experiments were 0.01, 0.10, 0.50, and 0.75. Debond lengths and fatigue cycles were monitored throughout each test. Tests were conducted at two or more constant amplitude stress levels to get several values of debond growth rates ( $da/dN$ ) from each specimen.

### D. TEST RESULTS:

1. Debond Measurement : The debond was measured as it grew over about 20 to 30 mm of length at each stress level during all test. The fatigue cycles were also recorded at each debond measurement. The measured data (debond length versus fatigue cycles) were fitted with a straight line or a polynomial curve using the regression analysis to get the debond growth rates,  $da/dN$ . Figures 3 and 4 show the typical relationships between the measured debond length and fatigue cycles. It can be seen in Figure 3 that fitting a straight line through the data points appears to be a reasonable average of the measured data. On the other hand, Figure 4 indicates a nonlinear relationship between debond length and the fatigue cycles. Therefore, the quadratic or higher order polynomial as

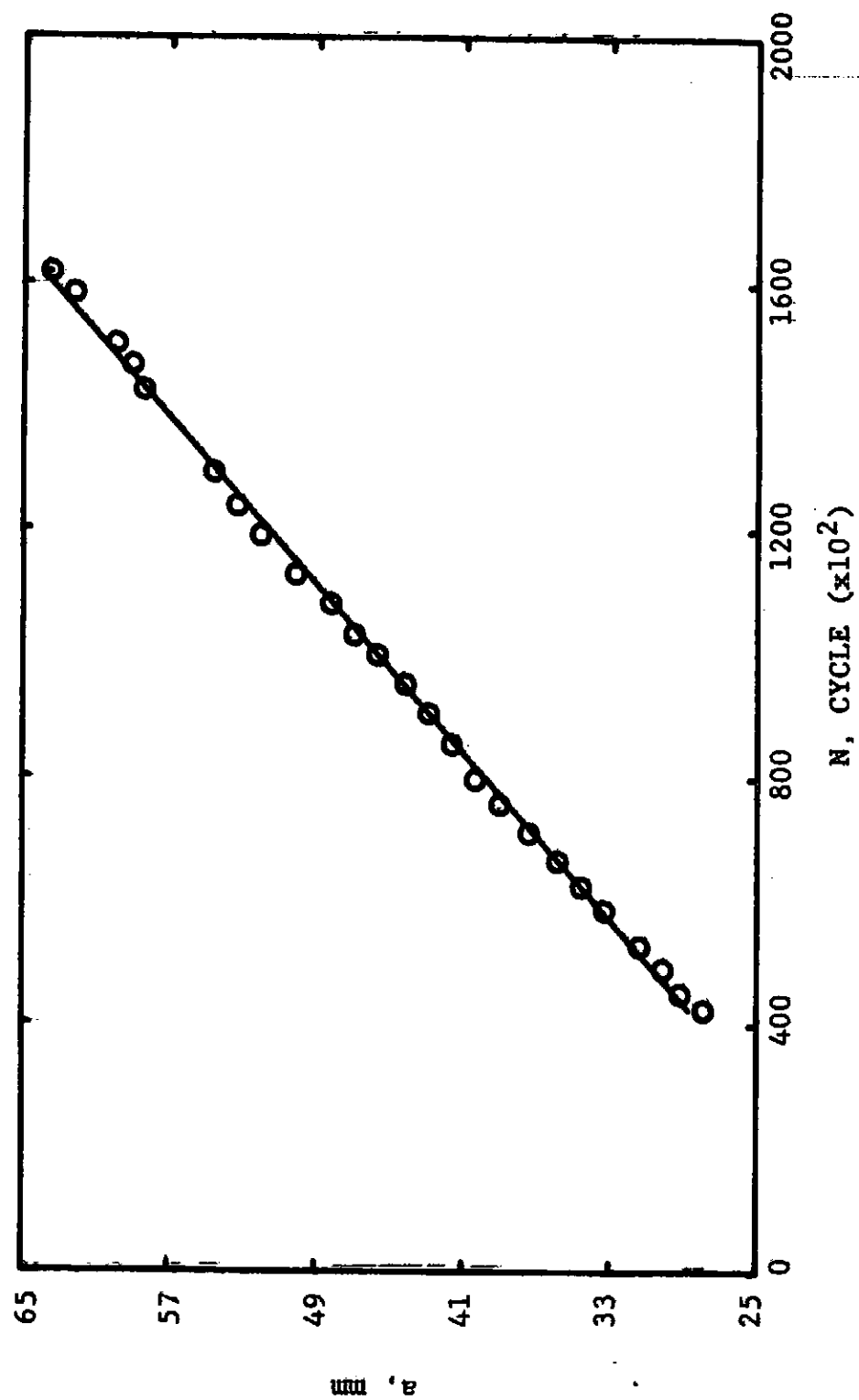


Figure 3. Linear Variation of Debond Growth with Fatigue Cycle for a Thin Strap (32/16) Specimen at 131 MPa Stress



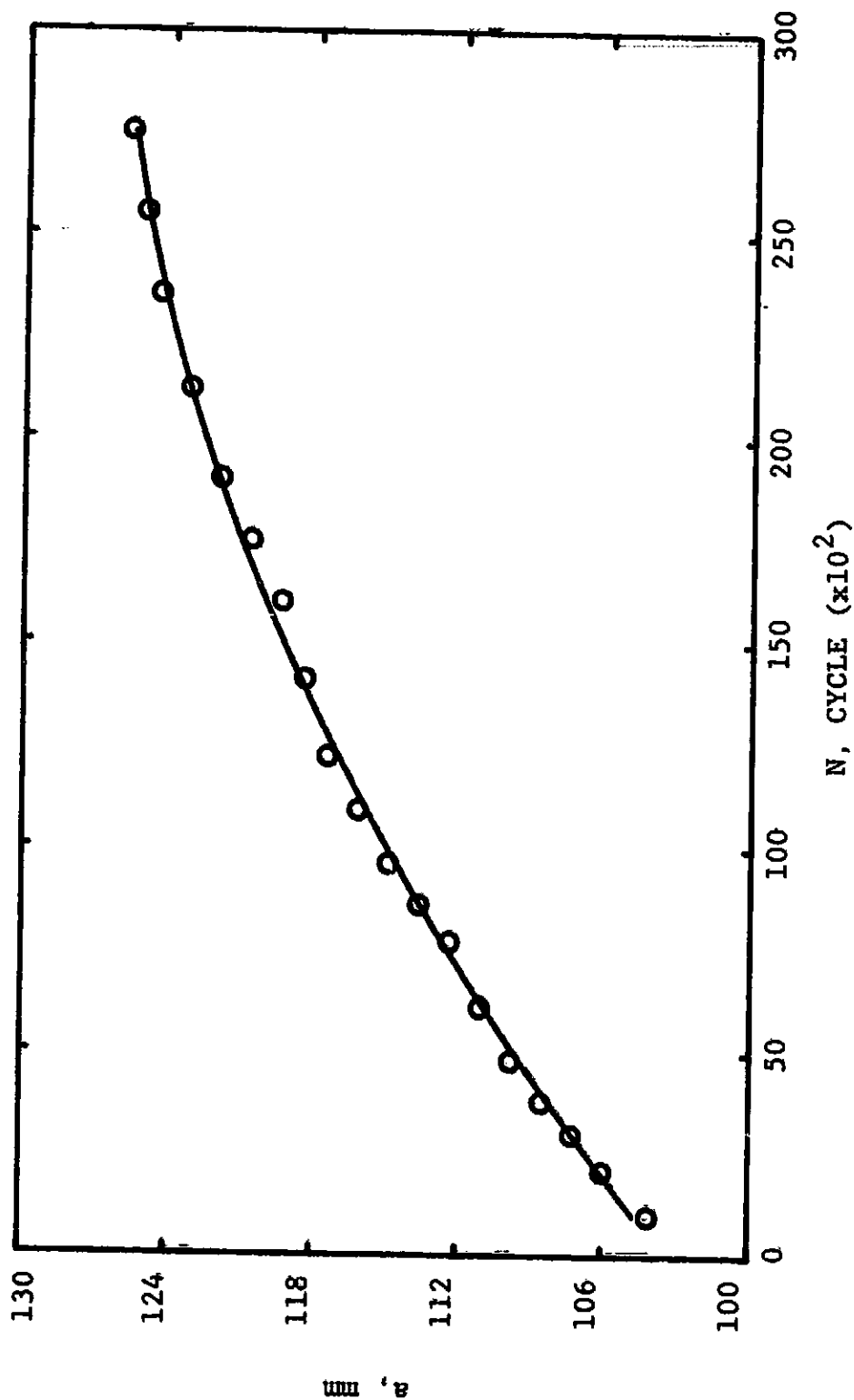


Figure 4. Nonlinear Variation of Debond Growth with Fatigue Cycle for a Thin Strap (32/16) Specimen at 140 MPa Stress

shown in the figure 4 is a reasonable representation of the measured data. Figure 5 shows the measured debond length as a function of fatigue cycles for different stress levels for a thin strap (32/16) specimen. The detailed explanation of these test results will be discussed in a later chapter entitled "Finite Element Analysis".

2. Debond Surfaces : Possible fatigue failure modes in a bonded joint are cyclic debonding, delamination, adherend fatigue, or a combination of these. In this study, the primary failure of all specimens occurred by cyclic debonding of the adhesive. On close examination of the debond surfaces, it was found that more adhesive remained on the lap than on the strap adherend. Also, there was some  $0^\circ$  fiber pull-off from the strap adherend. Figure 6 shows typical debond surfaces with such failures. These observed characteristics of debond surface in the present study are very similar to as found in the previous study. (6) A detailed explanation of this debond behavior will be discussed in the chapter entitled "Finite Element Analysis".

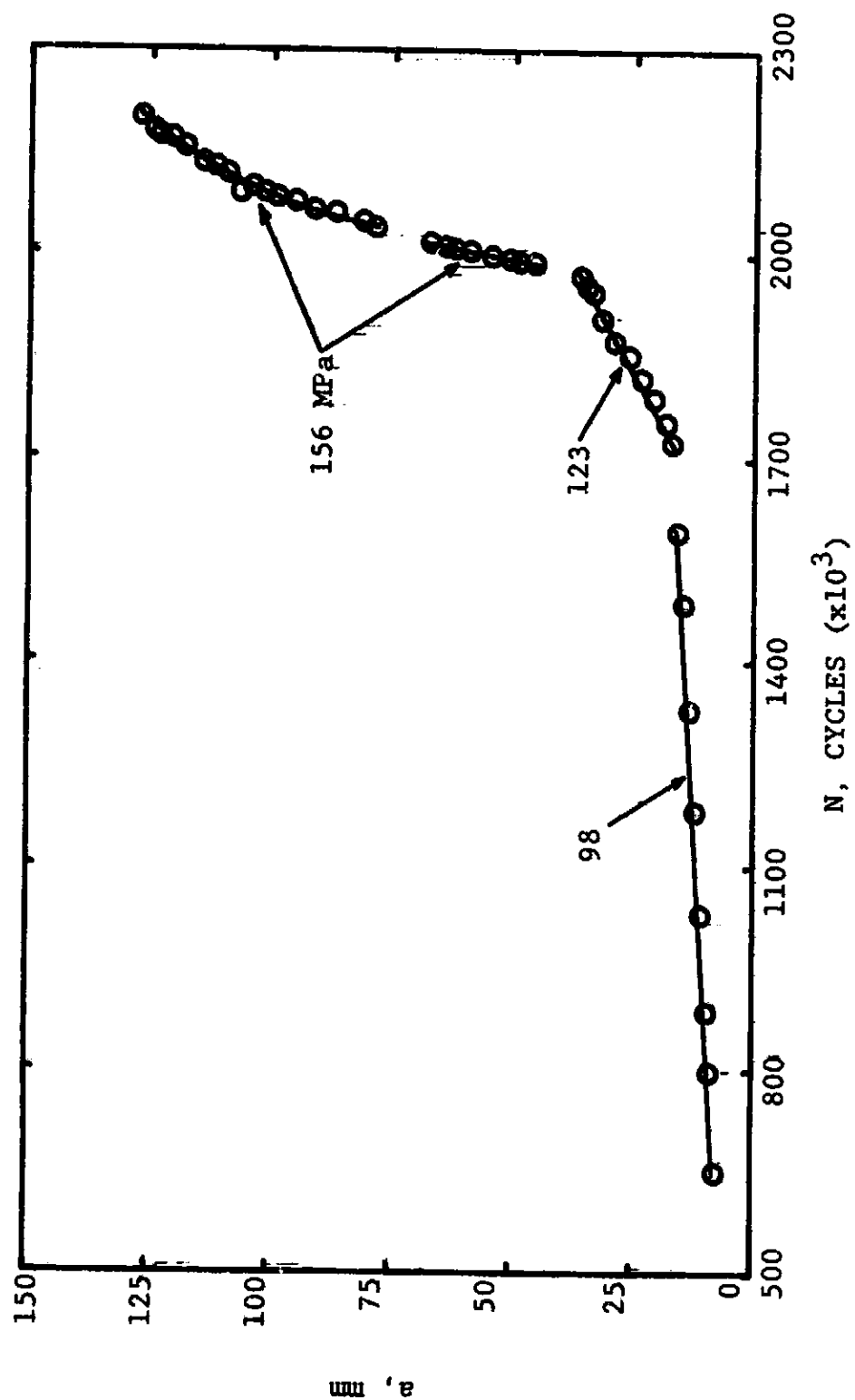


Figure 5. Typical Debond Growth Data at Different Stress Levels for a Thin Strap (32/16) Specimen

ORIGINAL PAGE IS  
OF POOR QUALITY

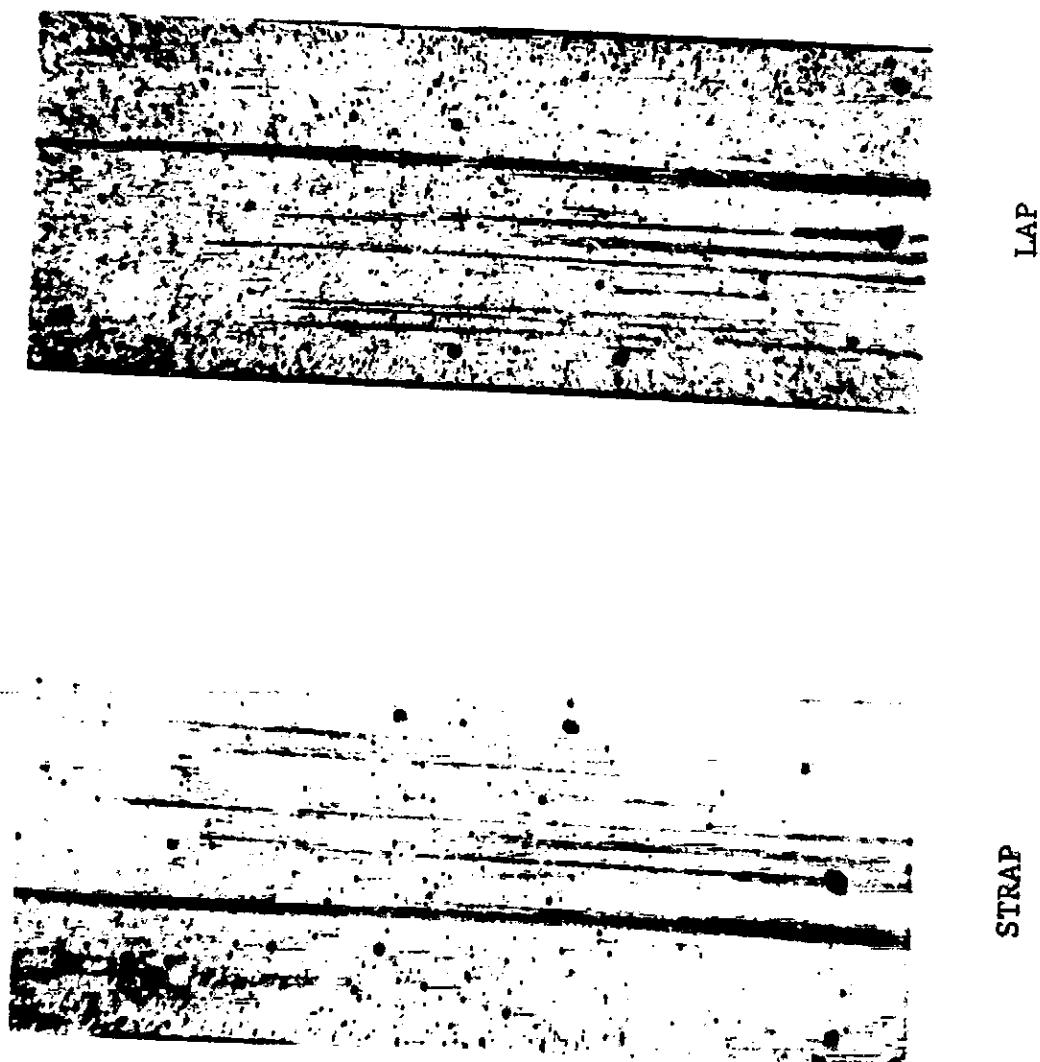


Figure 6. Debonded Surfaces of Cracked Lap Shear Specimen  
with 32 Ply Strap and 16 Ply Lap

#### IV. FINITE ELEMENT ANALYSIS

Previous studies of debonding propagation in adhesively bonded joints have shown that the fracture mechanics concept of the strain energy release rate is a useful tool for understanding their mechanics.<sup>(3,4)</sup> A two dimensional finite element stress analysis program called GAMNAS<sup>(17)</sup> was used to calculate the strain energy release rates for all cracked lap shear specimens. This program accounts for the geometric nonlinearity associated with the large rotations that often occur in the cracked lap shear specimen.

The tested cracked lap shear joint was analyzed by a finite element model which typically contained approximately 1600 isoparametric four-node elements and 3000 degrees of freedom. A finite element model along with the accompanying boundary conditions are shown in Figure 7. In the finite element model each ply of composite was modeled as a separate layer except for the 0° ply at the adhesive interface which was modeled in two or more layers. Plane strain conditions were assumed in the analysis. The strain energy release rates were calculated using a virtual crack closure technique.<sup>(20)</sup> In the analysis of cracked lap shear specimens, the calculation of strain energy release rates depends on four parameters: 1) boundary condition, 2) debond location, 3) load level, and 4) debond length. These are discussed separately in the following.

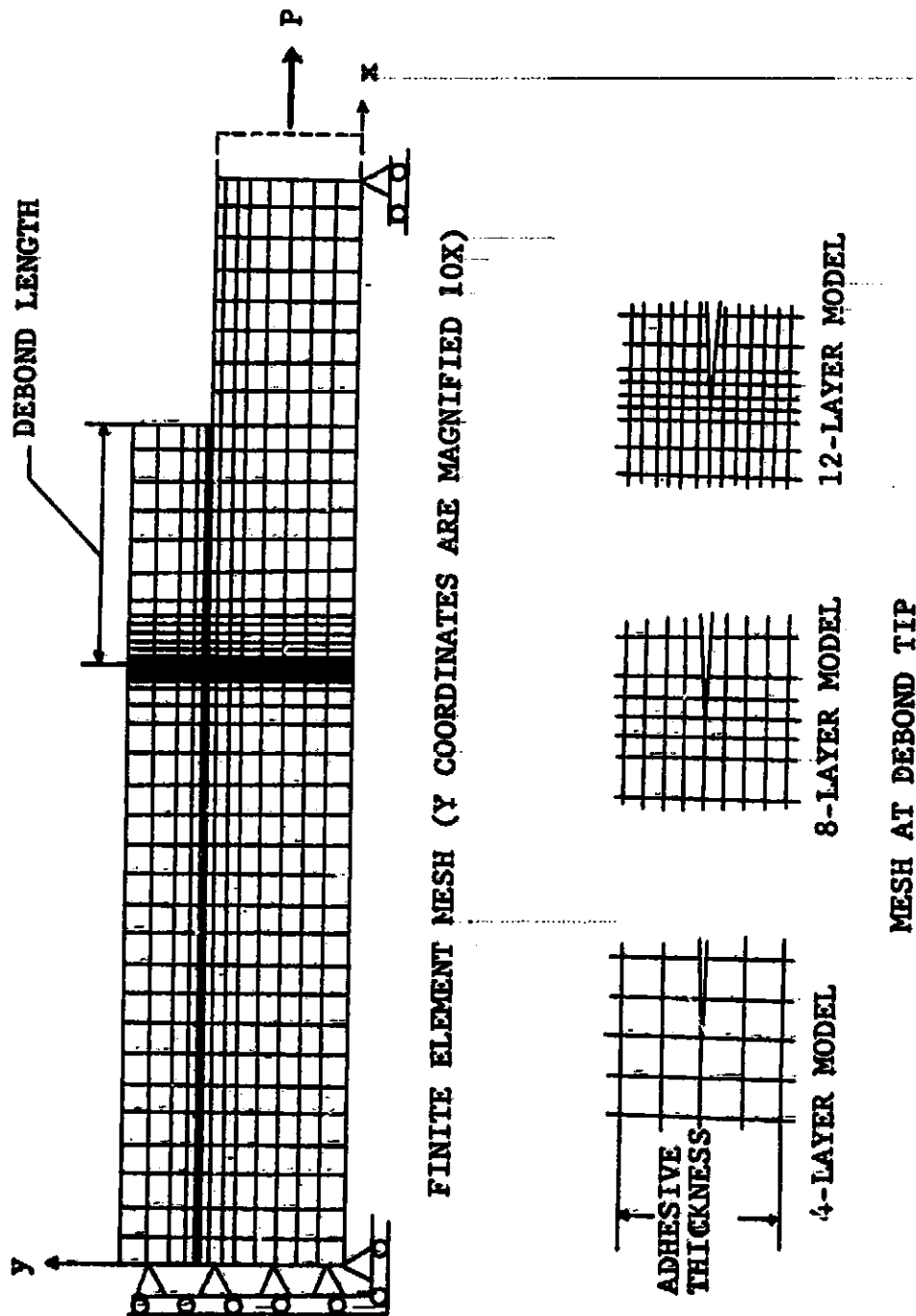


Figure 7. Finite Element Model

#### A. BOUNDARY CONDITION

The boundary condition applied to the cracked lap shear specimen in the present FEM analysis is shown in Figure 7. A multipoint constraint was imposed to prevent rotation of the loaded end of the model and to apply the equal axial displacements to simulate the grip conditions of test machine. To verify the validity of the boundary condition employed in the FEM analysis, the lateral deflection was measured with the extensometer for a thick strap specimen with crack length of 50.8 mm. The measured deflection was compared with the calculated deflection from FEM analysis (with boundary conditions as shown in Figure 7) in Figure 8 which are in good agreement with each other.

Further, experimental investigation showed that a slight displacement (i.e. 0.00355 mm) occurred in the y-direction at left edge of the CLS specimen. This was due to the lateral deflection of the grip attached to the hydraulic actuator. The other grip attached to the load cell had no such displacement. In order to determine the effect of this displacement on the analytical calculation of strain energy release rates, the measured lateral displacement was applied in the FEM analysis. The FEM results are compared with and without this lateral deflection in Table III. In fact, this displacement of specimen did have the negligible effect on the calculations of strain energy release rates. Therefore, the boundary condition, as shown in Figure 7, was appropriate and hence used in all calculations.

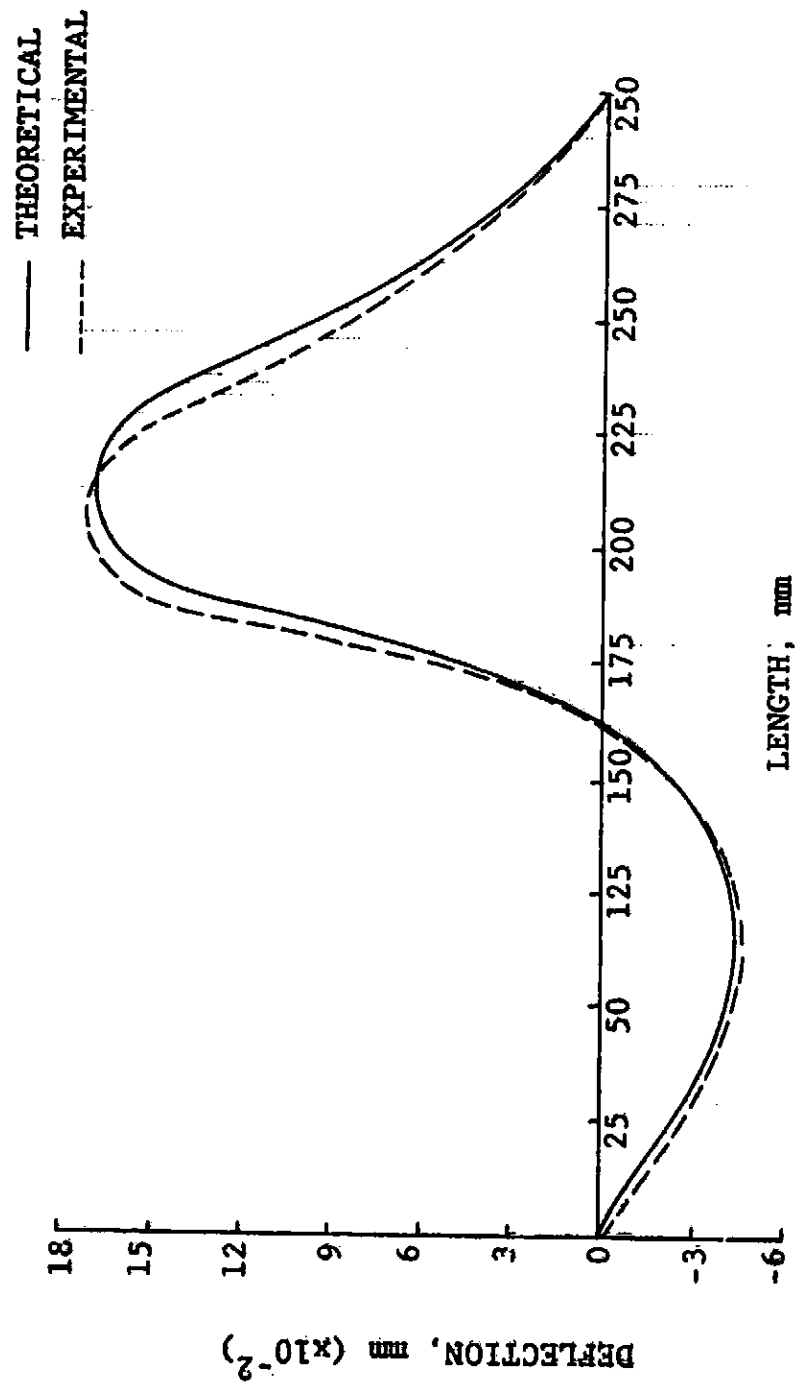


Figure 8. Lateral Deflection of a Thick Strap (16/32) Specimen with a Crack Length of 50.8 mm at 82 MPa Stress



TABLE III

EFFECT OF LATERAL DEFLECTION ON  $G$  CALCULATION  
OF THICK STRAP (16/32) SPECIMEN WITH CRACK  
LENGTH OF 50.8 mm AT 82 MPa STRESS

	$G_I$	$G_{II}$ (J/m <sup>2</sup> )	$G_T$
With Disp.	29.009	139.081	168.091
Without Disp.	29.044	139.130	168.175

## B. DEBOND LOCATION

As mentioned previously in chapter III, the debond grew adjacent to the strap adherend interface in all tests. It was very difficult to physically measure the exact location of the debond. However, the debond generally grew within one-fourth of the total adhesive thickness away from the strap interface. The influence of debond location on strain energy release rates was studied using GAMNAS<sup>(17)</sup> in the thick strap (16/32) cracked lap shear specimen. For this purpose, the adhesive thickness was modeled with 4, 8, and 12 layers of elements, as shown in Figure 7. The variation of calculated strain energy release rates  $G_T$ ,  $G_I$ , and  $G_{II}$  with the location of debond within the thickness of the EG-3445 adhesive is shown in Figure 9. This figure clearly indicates: 1) total strain energy release rate,  $G_T$ , remains constant for all locations of the debond; 2) mode I strain energy release rate,  $G_I$ , reaches its maximum value near the adhesive strap interface; and 3) mode II strain energy release rate,  $G_{II}$ , reaches its maximum value near the adhesive lap interface. The debond always initiated and grew in the region of highest  $G_I$ . This is consistent with theoretical results and experimental observations that  $G_I$  has greater influence on the debond location in the adhesive joint. In addition, Figure 9 shows that 4 layer model is adequate to accurately evaluate  $G_T$ , while a refined model is required to evaluate  $G_I$  and  $G_{II}$ . Thus, the 12-layer model was used in the FEM of the present study.

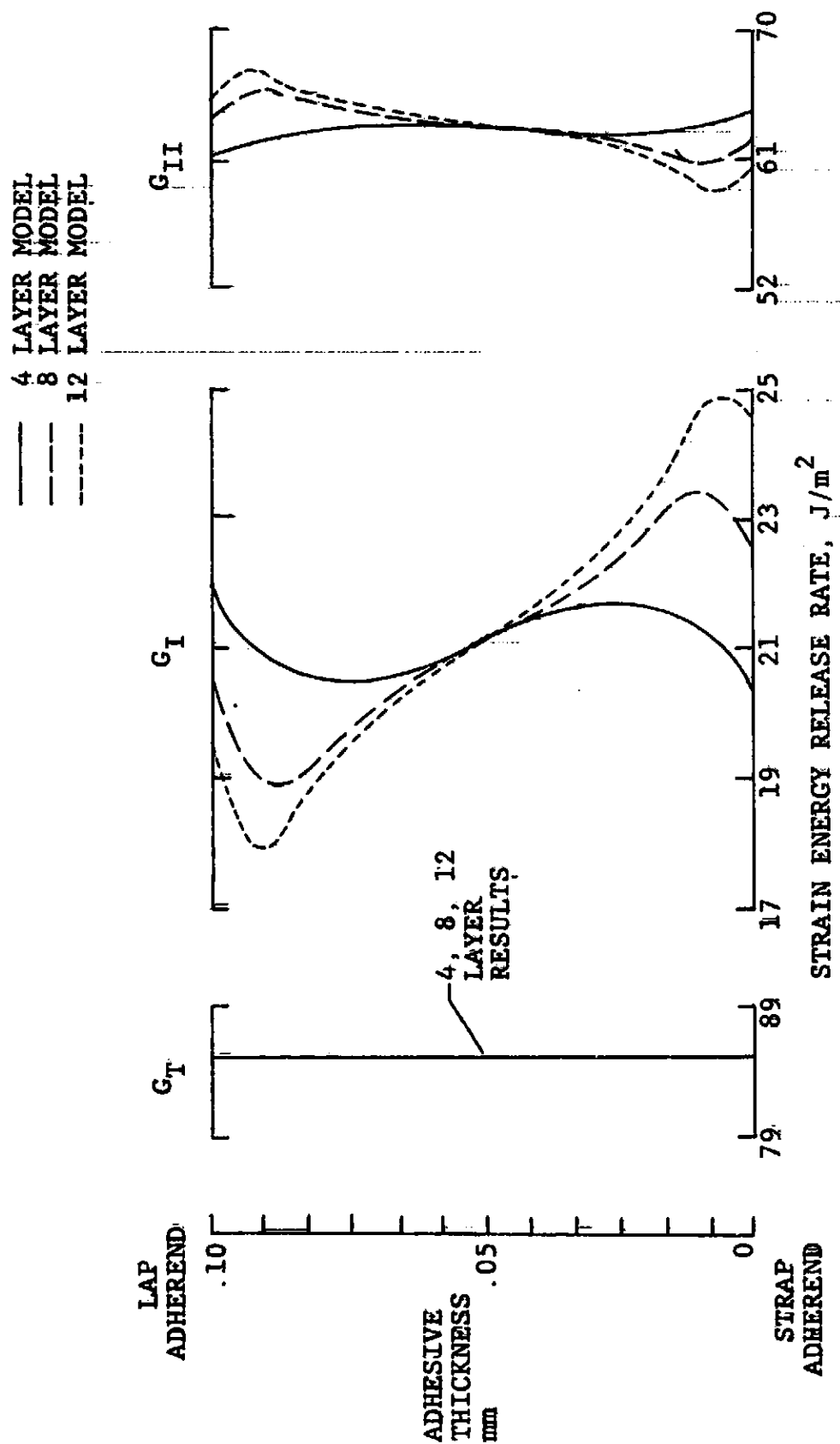


Figure 9. Variation of Strain Energy Release Rate with Location of Debond within Adhesive for Thick Strap (16/32) Specimen at 82 MPa Stress

In order to analyze the experimental debond growth rates, the debond location was selected by engineering judgement to be at one-sixth of the adhesive thickness away from the adhesive strap interface. This was also consistent with the previous study by Mall et al. (6)

### C. LOAD LEVEL

Figure 10 shows the variation of strain energy release rates  $G_I$  and  $G_{II}$  with the applied strap stress for thick strap (16/32) cracked lap shear specimen with crack length of 50.8 mm obtained from the geometric nonlinear finite element analysis. Also, these are presented in Table IV which shows that the  $G_I$  and  $G_{II}$  from non-linear analysis are functions of the square of applied stress within five percent upto the maximum stress employed in the present study.

### D. DEBOND LENGTH

Both thick strap (16/32) and thin strap (32/16) specimens were analyzed to determine the variation of strain energy release rates,  $G_I$ ,  $G_{II}$ , and  $G_T$  with debond length. Figure 11 shows the typical variation of  $G_T$  and  $G_I$  to  $G_{II}$  ratio with debond length for two cracked lap shear specimens used in the present study. As mentioned previously, Figure 3 and 4 showed a linear and non-linear relationship between the measured debond length and fatigue cycles respectively. It can be seen by comparing Figures 3 and 11 that a linear

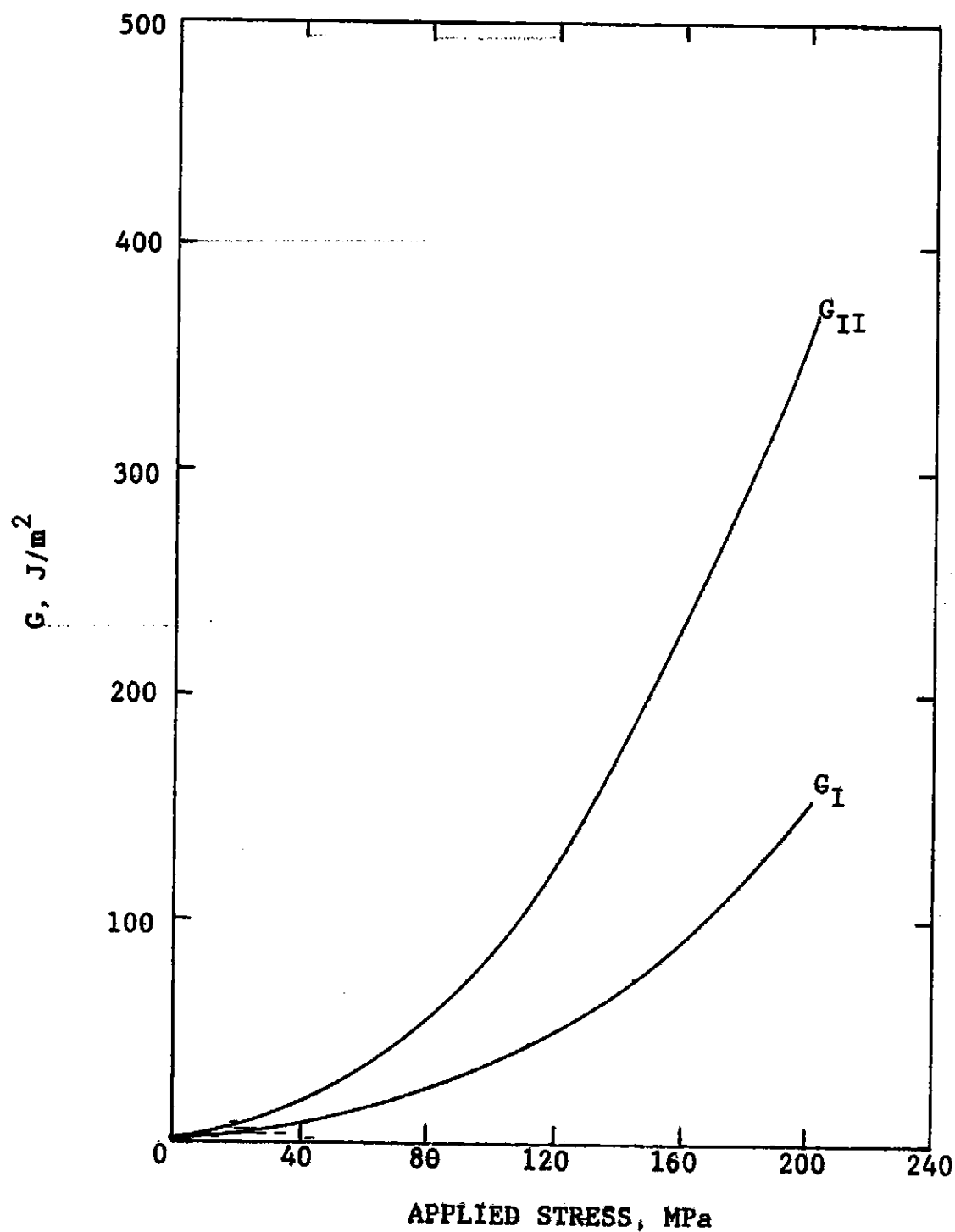


Figure 10. Variation of Strain Energy Release Rates with Applied Stress for Thick Strap (16/32) Specimen with a Crack Length of 50.8 mm

TABLE IV

VARIATION OF STRAIN ENERGY RELEASE RATE WITH  
 APPLIED STRESS FOR THICK STRAP (16/32)  
 SPECIMEN WITH CRACK LENGTH OF 50.8 mm

Applied Stress (KPa)	Non-linear		Linear	
	$G_I$	$G_{II}$	$G_I$	$G_{II}$
	(J/m <sup>2</sup> )		(J/m <sup>2</sup> )	
41042	5.820	15.656	6.294	16.466
82083	23.179	60.919	25.175	65.861
123125	52.778	135.084	56.644	148.189
164167	95.706	238.140	100.701	263.448
205208	153.027	370.457	157.344	411.634

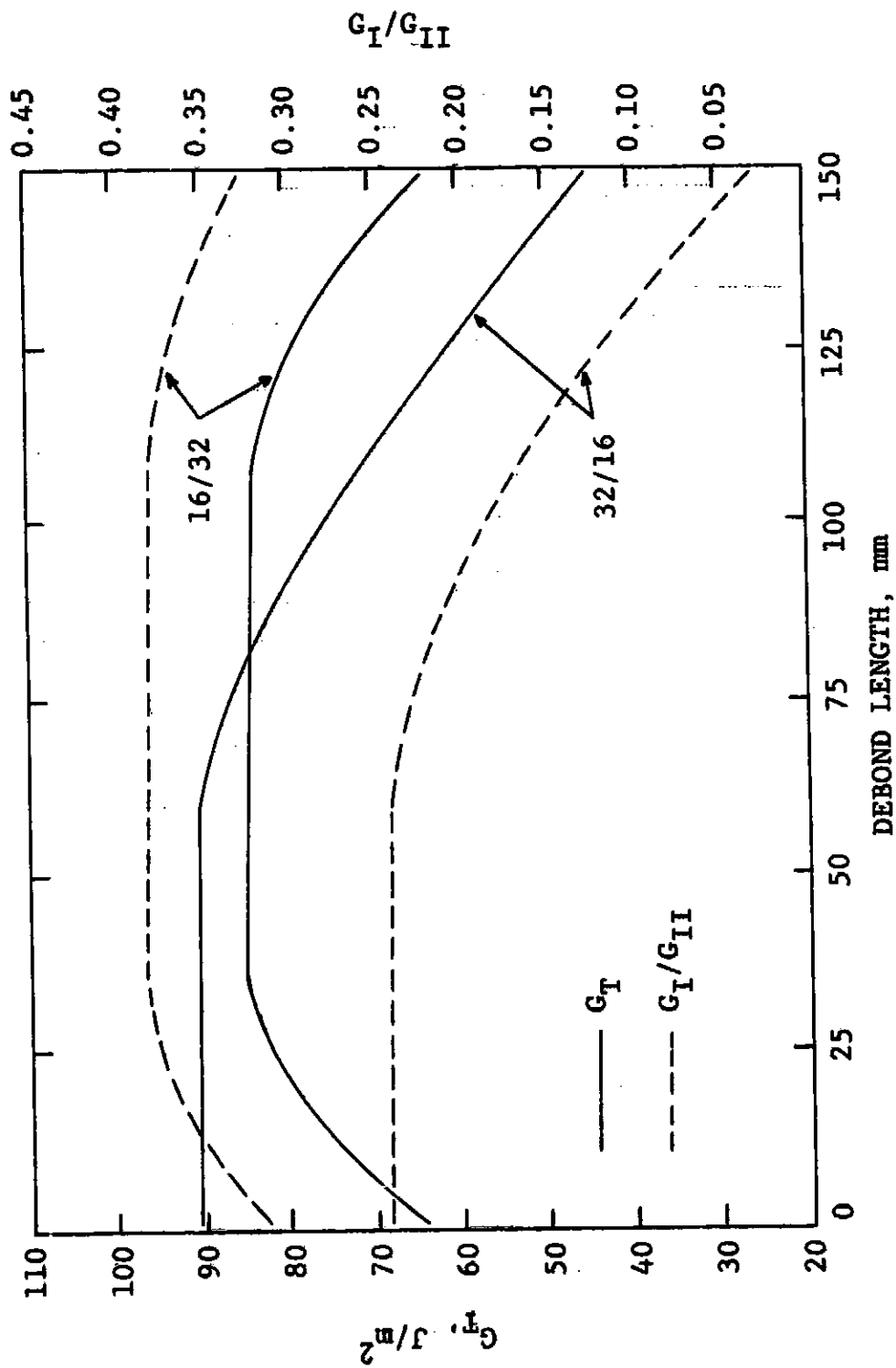


Figure 11. Variation of Strain Energy Release Rates with Debond Length for Thick and Thin Strap Specimens

relationship between the measured debond length versus fatigue cycles was observed where the strain energy release rates were constant with the crack length. Similarly, comparison of Figures 4 and 11 shows that a non-linear relationship between the measured debond length versus fatigue cycles was found where the strain energy release rates were not constant with the crack length.



## V. RESULTS AND DISCUSSION

As mentioned in the introduction, the objective of the present study was; 1) to understand the interaction of mixed-mode loading and 2) the effect of stress ratio on cyclic debonding in adhesively bonded composite joints. The results of the present study will be discussed in these contexts in the following.

### A. THE INTERACTION OF MIXED-MODE LOADING ON CYCLIC DEBONDING

Debond growth rates were calculated from the measured debond length and fatigue cycles as discussed in the chapter entitled "Experiment". The corresponding strain energy release rates  $G_I$ ,  $G_{II}$ , and  $G_T$  were calculated using finite element analysis of cracked lap shear specimen as discussed in the chapter entitled "Finite Element Analysis". The measured debond growth rates are expressed as the function of the corresponding strain energy release rates  $G_I$ ,  $G_{II}$ , and  $G_T$  as shown in Figures 12, 13, and 14, respectively. The corresponding relations obtained from the CLS specimens in the previous study<sup>(6)</sup> are also shown in Figures 12, 13, and 14 as solid line instead of data points for the sake of clarity. The two geometries of cracked lap shear specimens, in the present study, consisted of 16 plies lap bonded to 32 plies strap and 32 plies lap bonded to 16 plies strap, and in the

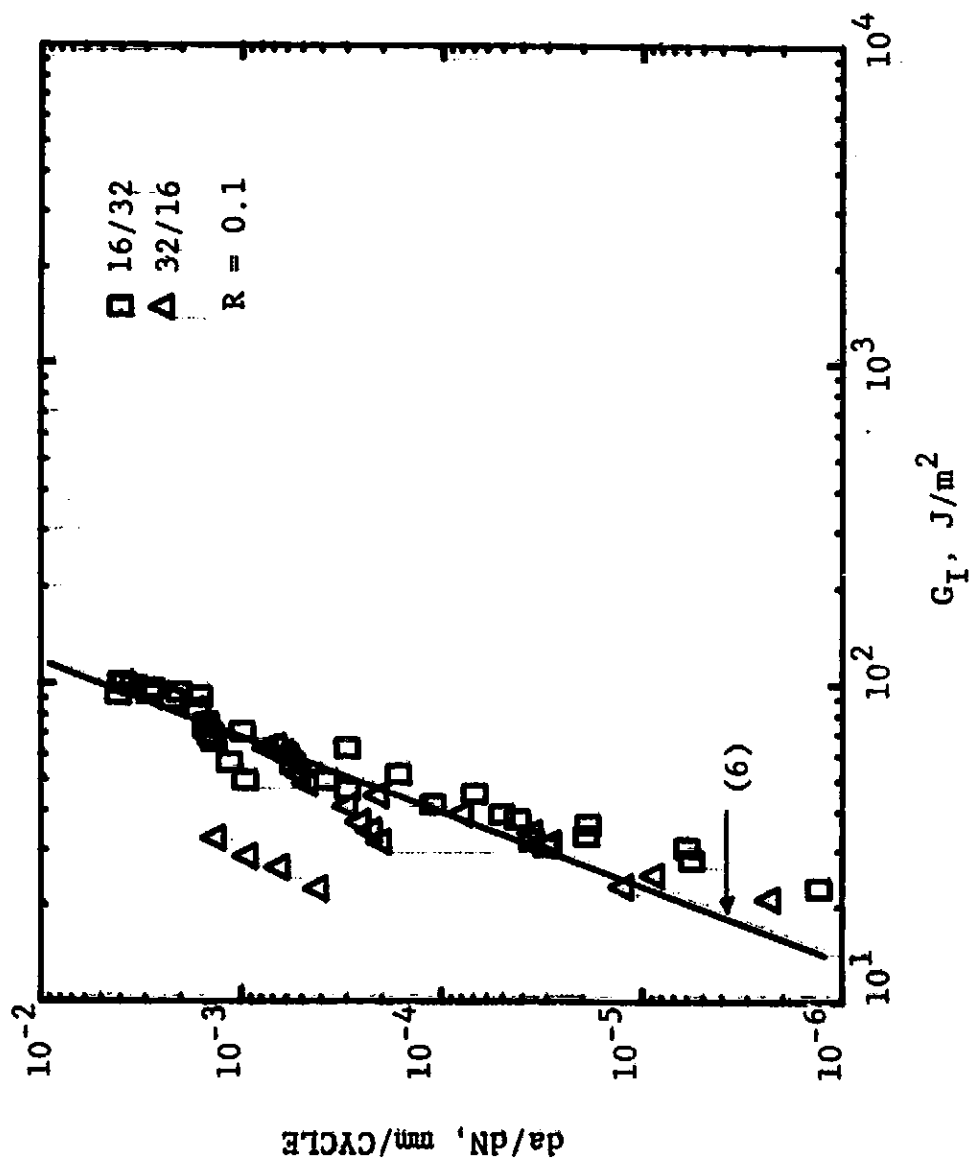


Figure 12. Comparison of Relationship Between  $G_I$  Versus Debond Growth Rate

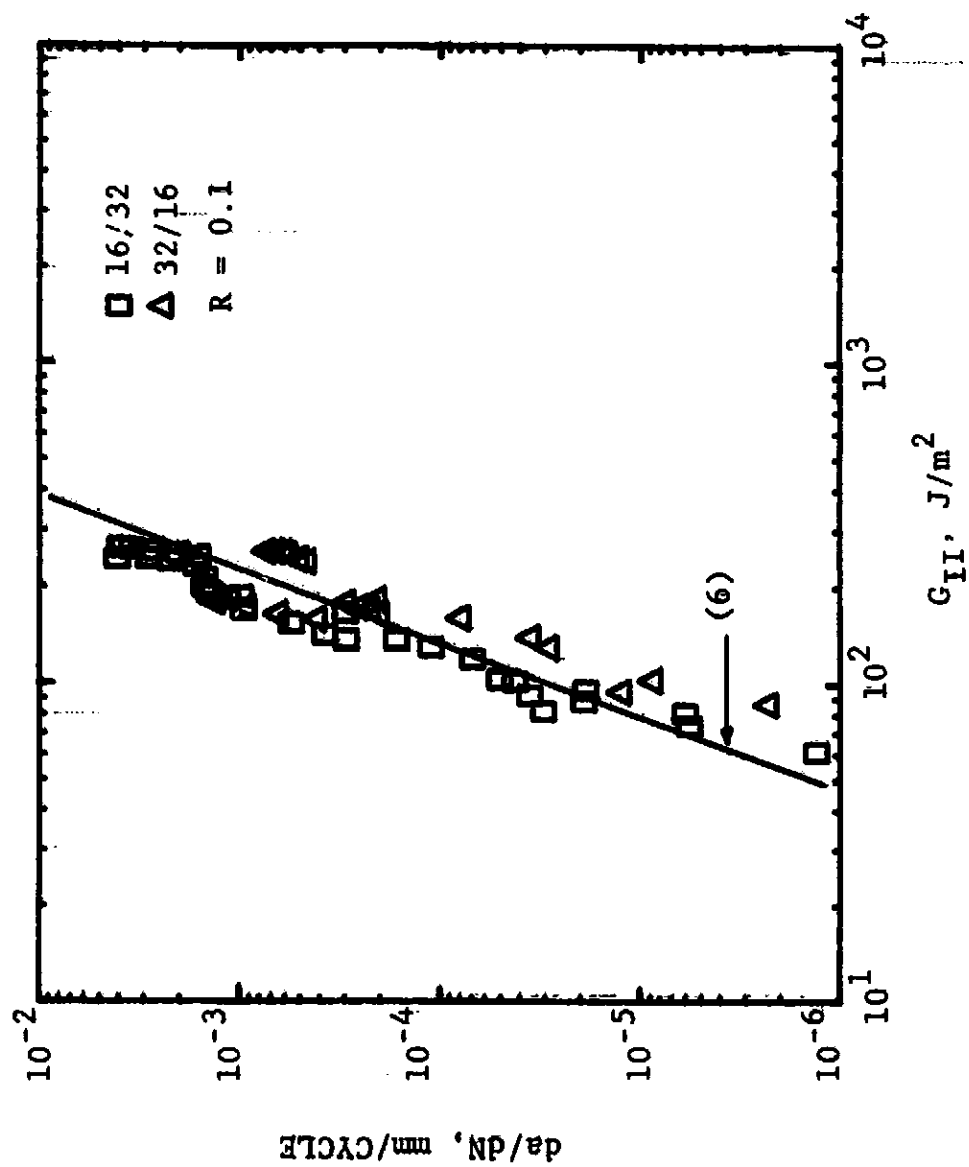


Figure 13. Comparison of Relationship Between  $G_{II}$  Versus Debond Growth Rate

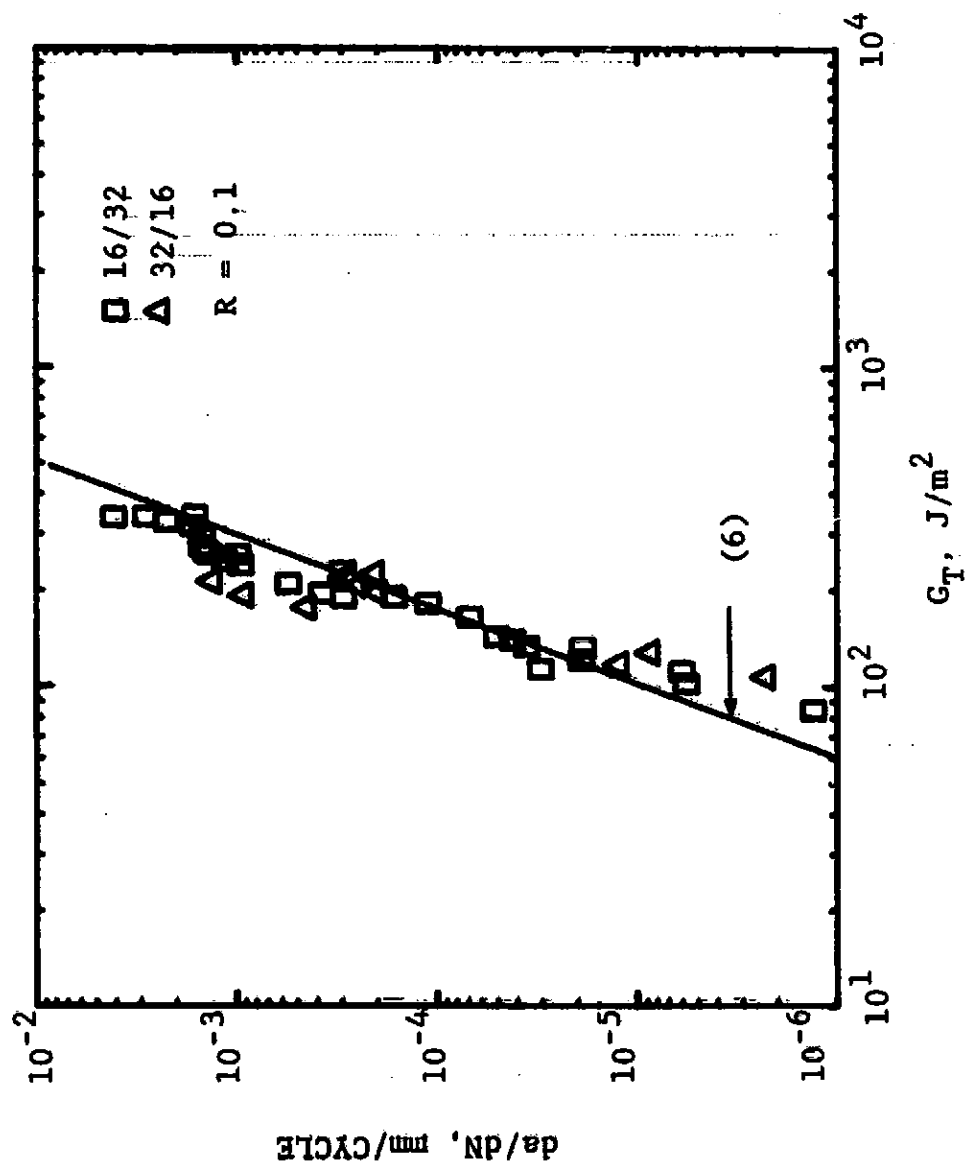


Figure 14. Comparison of Relationship Between  $G_T$  Versus Debond Growth Rate

previous study<sup>(6)</sup>, specimens consisted of 8 plies lap bonded to 16 plies strap and 16 plies lap bonded to 8 plies strap. The  $G_I$ ,  $G_{II}$ , and  $G_T$  versus  $da/dN$  relations from present and previous studies<sup>(6)</sup> are in good agreement with each other.

Figures 12, 13, and 14 indicate that the data from different specimen geometries are within an acceptable scatter band as similarly observed in fatigue crack propagation in metals. This means that specimen geometry did not influence the relationship between the debond growth rate and total strain energy release rate,  $G_T$ . Furthermore, the cyclic debond growth rates for a given bonded system are reproducible from one specimen to another within a scatter band comparable to that for fatigue crack growth in metals.

To determine the interaction of each component of mixed-mode loading on cyclic debonding, the measured debond growth rates obtained from two geometries of CLS specimens were correlated with strain energy rates (i.e.  $G_I$ ,  $G_{II}$ , and  $G_T$ ). This correlation is shown in Figures 15, 16, and 17 where a power law relationship of the form

$$da/dN = c(G)^n$$

was fitted to the data using a linear regression analysis. This relation is shown as a solid line in Figures 15, 16, and 17. The values of  $c$  and  $n$ , as well as the correlation coefficient are also shown in these figures. Since the

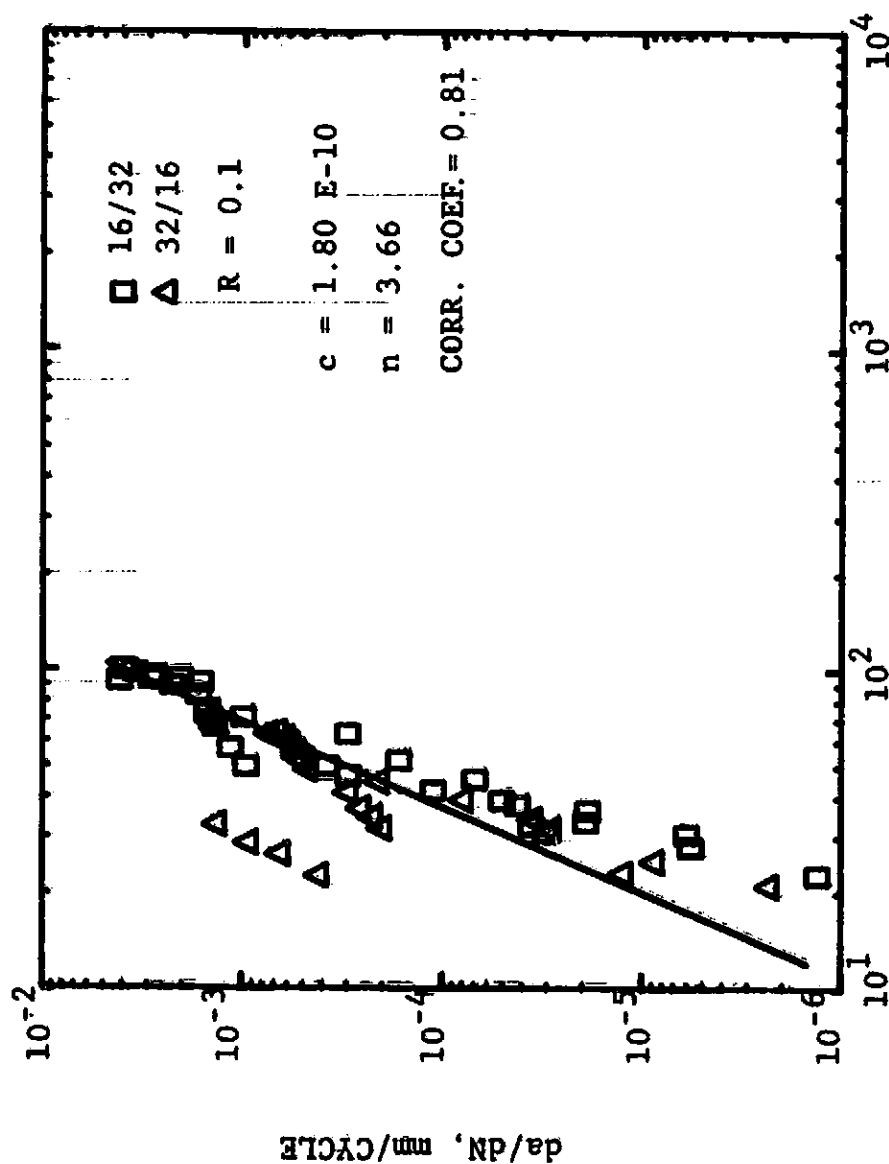


Figure 15. Relation Between  $G_T$  and Debond Growth Rate

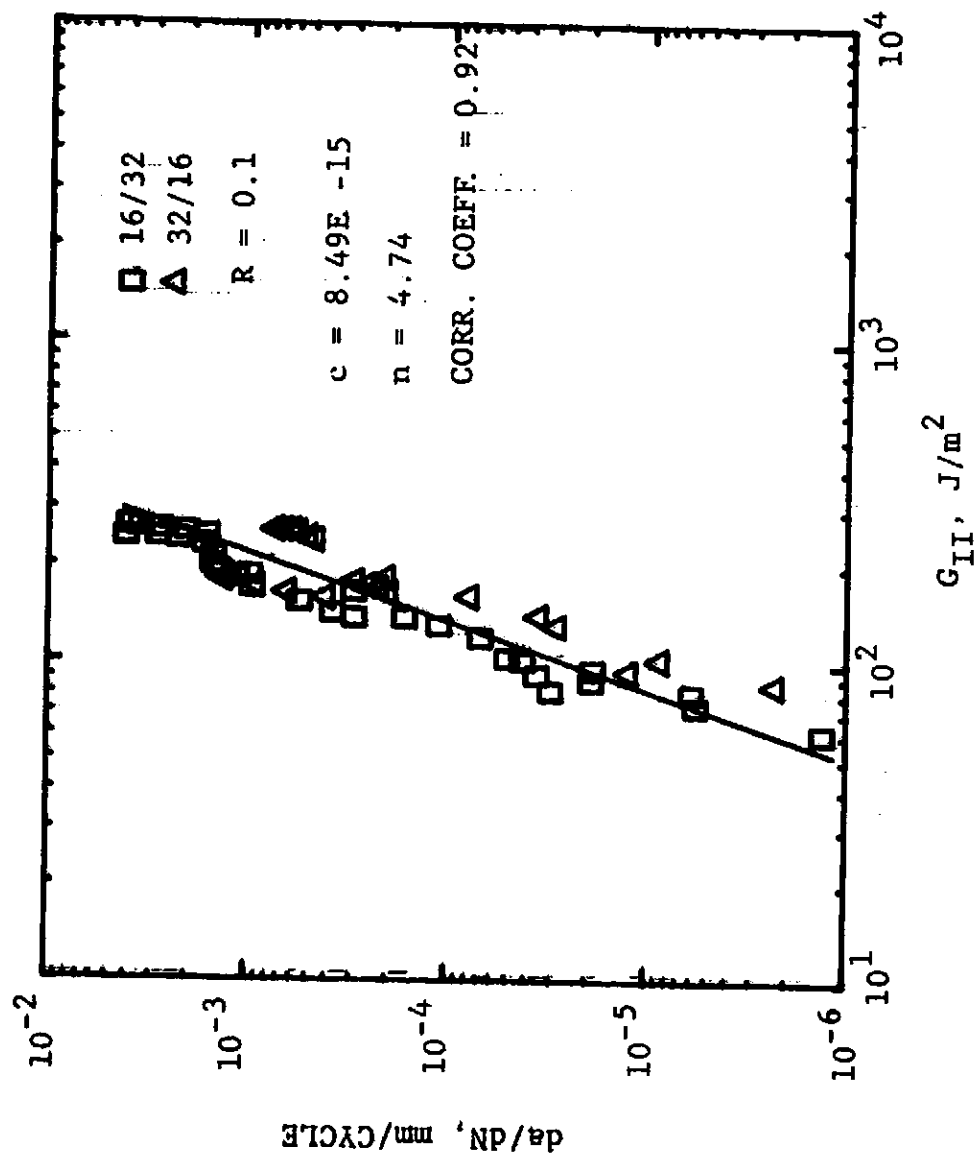
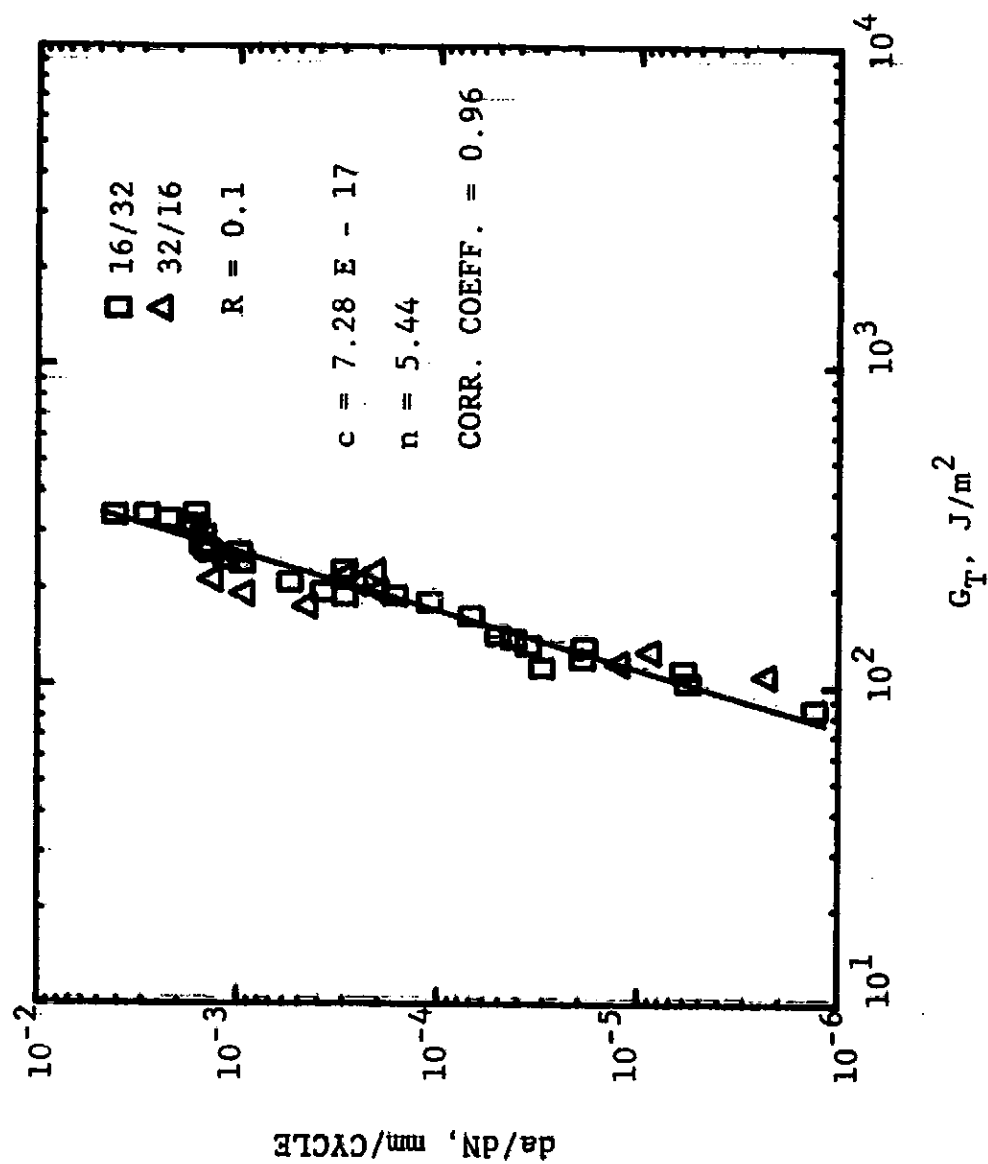


Figure 16. Relation Between  $G_{II}$  and Debond Growth Rate

Figure 17. Relation Between  $G_T$  and Debond Growth Rate



correlation coefficient closer to 1 is the indication of better correlation, the  $G_T$  correlated the debond growth rate better than either  $G_I$  or  $G_{II}$ . This shows that the total strain energy release rate is the driving parameter for the cyclic debonding under mixed-mode loading. This was also found in the previous study by Mall et al.<sup>(6)</sup>, where the tested specimens provided a narrow range of  $G_I/G_{II}$  (i.e. ranging from 0.25 to 0.31) while in the present study, a wide range of  $G_I/G_{II}$  ranging from 0.03 to 0.38 was obtained. The  $G_I/G_{II}$  in the present study is very close to that experienced by the actual bonded joints in practical applications. Furthermore, Mall et al.<sup>(7)</sup> also studied the cyclic debonding of double cantilever beam (DCB) specimens under opening mode I loading. This showed that the relation  $G_I$  versus  $da/dN$  from the DCB specimen under opening mode I load did not agree with the relation  $G_I$  versus  $da/dN$  from the CLS specimen. However, the relation  $G_I$  versus  $da/dN$  from DCB specimens agreed with the relation  $G_T$  versus  $da/dN$  from the CLS specimen. Thus, this confirmed that the cyclic debond failure is a function of total strain energy release rate.

The present study along with the previous studies<sup>(6,7)</sup>, thus, provided the debond growth rate measurements under various load conditions: mode I loading, mixed-mode I and II loading and almost mode II loading. The results of these studies led to the following conclusion; the total strain energy release rate is the governing factor for cyclic

debonding of adhesively bonded composite joints under in-plane mixed-mode loading.

#### B. THE EFFECT OF STRESS RATIO ON CYCLIC DEBONDING

To determine the influence of stress ratio, the measured debond growth rates were correlated with total strain energy release rate,  $G_T$ , and total strain energy release rate range,  $\Delta G_T$ , (i.e.  $\Delta G_T = G_{\max} - G_{\min}$ ) as shown in Figures 18 and 19, respectively. It can be seen in Figure 18 that the relationship between  $G_T$  and  $da/dN$  is different for each stress ratio. On the other hand, Figure 19 shows that the relation between  $\Delta G_T$  and  $da/dN$  is the same with different stress ratios. This shows that  $\Delta G_T$  is the driving parameter for cyclic debonding of adhesively bonded joints when subjected to cyclic loads with different ratio (i.e. ratio of minimum to maximum load of the fatigue cycle). Hence, the power law relation as given by

$$da/dN = c(\Delta G_T)^n$$

takes into the account of the stress ratio effect in characterizing the mechanics of cyclic debonding. Furthermore, Figure 19 shows that data from different stress ratios are within an acceptable scatter band.

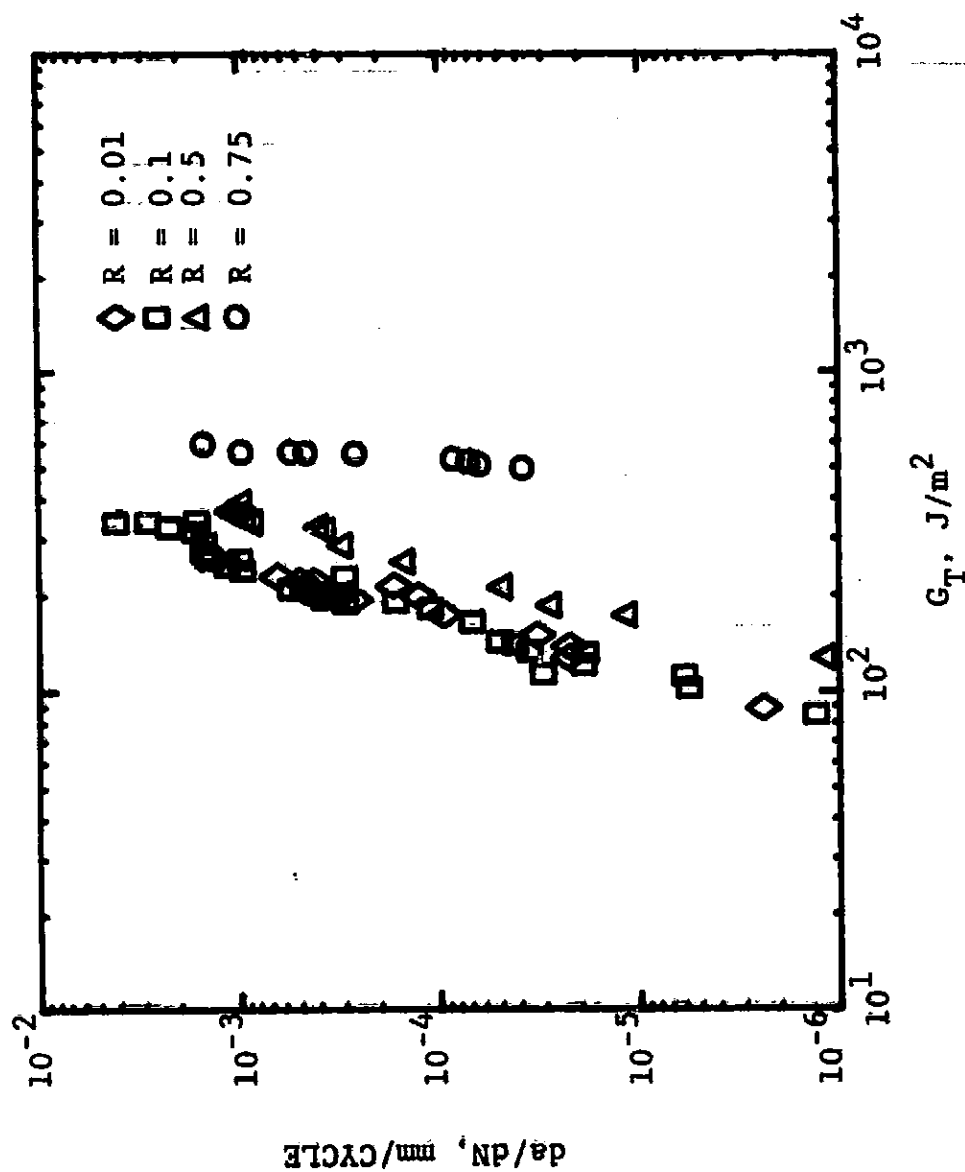


Figure 18. Effect of Stress Ratio on the Relation Between Total Strain Energy Release Rate and Debond Growth Rate

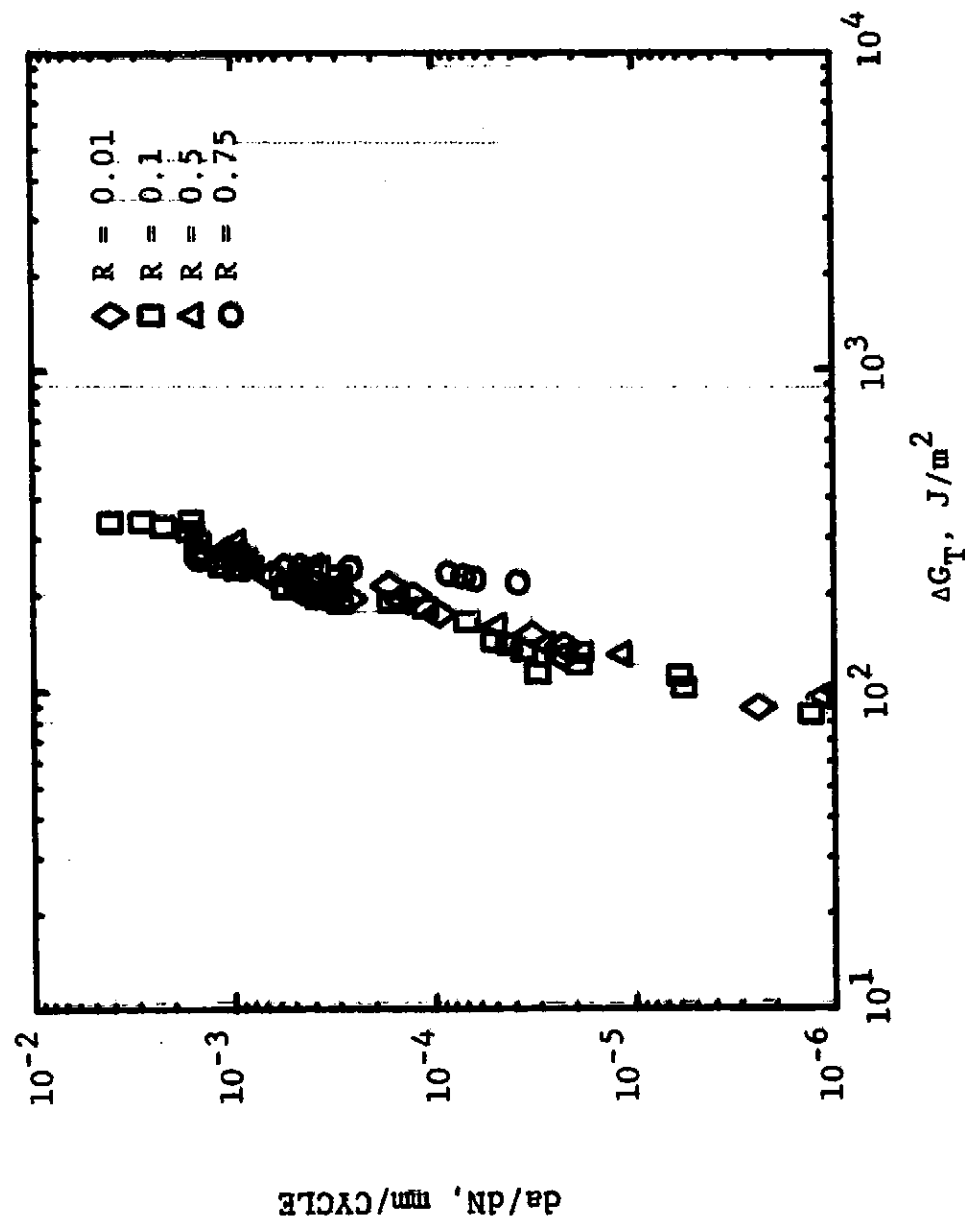


Figure 19. Effect of Stress Ratio on the Relation Between Total Strain Energy Release Rate Range and Debond Growth Rate

## VI. CONCLUSIONS

A combined experimental-analytical investigation of composite-to-composite bonded joint was undertaken to assess: 1) the influence of each components of strain energy release rates (i.e.  $G_I$ ,  $G_{II}$ , or  $G_T$ ) on cyclic debonding under mixed-mode loading; 2) the effect of stress ratio on debond growth rates. Several cracked lap shear specimens consisting of graphite/epoxy adherends bonded with EC-3445 adhesive were studied under mixed-mode cyclic loading. The following conclusions were obtained:

1. Cracked lap shear specimens provided consistent debond growth data. The cyclic debond growth rates were reproducible from one specimen to another within a scatter band comparable to that for fatigue crack growth in metals.
2. The governing factor for cyclic debond failure of adhesively bonded composite joints was found to be the total strain energy release rate,  $G_T$ .
3. The debond always grew in the region of the adhesive strap interface where the highest mode I loading occurred. This indicates that  $G_I$  has greater influence on debond location.
4. The failure of cracked lap shear specimens occurred by cyclic debonding of adhesive, accompanied by some  $0^\circ$  fiber pull-off from the strap adhered.

5. The total strain energy release rate range,  $\Delta G_T$ , was found to be the driving parameter for cyclic debonding of adhesively bonded joint under cyclic loads with different stress ratios.

## BIBLIOGRAPHY

1. Matthews, F.L.; Kilty, P.F.; and Godwin E.W.; "A Review of the Strength of Joints in Fiber-Reinforced Plastics, Part 2--Adhesively Bonded Joints," Composites, Vol. 13, No. 1, pp. 29-35, 1982.
2. Hart-Smith, L.J.; "Analysis and Design of Advanced Composite Bonded Joints," NASA CR-2218, National Aeronautics and Space Administration, 1974.
3. Roderick, G.L.; Everett Jr., R.A.; and Crews Jr., J.H.; "Cyclic Debonding of Unidirectional Composite Bonded to Aluminum Sheet for Constant Amplitude Loading," Fatigue of Composite Materials, ASTM STP 569, American Society for Testing and Materials, 1975.
4. Brussat, T.R.; Chiu, S.T.; and Mostovoy, S.; "Fracture Mechanics for Structural Adhesive Bonds," AFML-TR-163, Air Force Materials Laboratory, 1977.
5. Mostovoy, S.; and Ripling, E.J.; "Fracturing Characteristics of Adhesive Joints," Final Report of Naval Air Systems Command, Contract No. N00019-72-0250, December 1972.

6. Mall, S.; Johnson, W.S.; and Everett Jr. R.A.; "Cyclic Debonding of Adhesively Bonded Composites," NASA TM-84577, National Aeronautics and Space Administration, November 1982.
7. Mall, S.; and Johnson, W.S.; "Characterization of Mode I and Mixed-Mode Failure of Adhesive Bonds Between Composite Adherends," NASA TM-86355, February 1985.
8. Kinloch, A.J.; "Review the Science of Adhesion, Part 2-- Mechanics and Mechanisms of Failure," Journal of Materials Science, Vol. 17, pp. 617-651, 1982.
9. Roderick, G.L.; Everett Jr., R.A.; and Crews Jr., J.H.; "Cyclic Debonding of Unidirectional Composite Bonded to Aluminum Sheet for Constant Amplitude Loading," NASA TN D-8126, National Aeronautics and Space Administration, 1976.
10. Brussat, T.R.; and Chiu, S.T.; "Fatigue Crack Growth of Bondline Cracks in Structural Bonded Joints," Journal of Engineering Materials and Technology, Vol. 100, pp. 39-45, 1978.



11. Romanko, J.; Liechti, K.M.; and Knauss W.G.; "Integrated Methodology for Adhesively Bonded Joint Life predictions," AFWAL-TR-82-4139, Air Force Wright Aeronautical Laboratories, 1982.
12. Francis, E.C.; Hufferd, W.L.; Lemini, D.G.; Thompson, R.E.; Briggs, W.E.; and Parmerter, R.R.; "Time Dependent Fracture in Adhesive Bonded Joints," CSD 2769-1TR-02, Chemecal Systems Division, November 1982.
13. Everett Jr., R.A.; and Johnson, W.S.; "Repeatability of Mixed-Mode Adhesive Debonding," NASA TM-85753, National Aeronautics and Space Administration, February 1984.
14. Jablonski, D.A.; "Fatigue Craek Growth in Structural Adhesives," Journal of Adhesion, Vol. 11, pp. 125-143, 1980.
15. Renton, W.J. and Vinson, J.R.; "Fatigue Behavior of Bonded Joints in Composite Material Structures," Journal of Aircraft, Vol. 12, No. 5, pp. 442-447.
16. Everett Jr., R.A.; "The Role of Peel Stresses in Cyclic Debonding," NASA TM-84504, National Aeronautics and Space Administration, June 1982.

17. Dattaguru, B.; Everett-Jr., R.A.; Whitcomb, J.D.; and Johnson, W.S.; "Geometrically-Nonlinear Analysis of Adhesively Bonded Joints," NASA TM-84562, National Aeronautics and Space Administration, September 1982.
18. Johnson, W.S. and Mall, S.; "A Fracture Mechanics Approach for Designing Adhesively Bonded Joints," NASA TM-85694, National Aeronautics and Space Administration, September 1983.
19. Hughes, E.J. and Rutherford J.L.; "Evaluation of Adhesives for Fuselage Bonding," Report No. KD-75-74, The Singer Company, 1975.
20. Rybicki, E.F. and Kanninen, M.F.; "A Finite Element Calculation of Stress Intensity Factors by a Modified Crack Closure Integral," Engineering Fracture Mechanics, Vol. 9, No. 4, pp. 931-938, 1977.

# Standard Bibliographic Page

1. Report No. NASA CR-177991		2. Government Accession No.		3. Recipient's Catalog No.	
4. Title and Subtitle MIXED-MODE CYCLIC DEBONDING OF ADHESIVELY BONDED COMPOSITE JOINTS				5. Report Date October 1985	
				6. Performing Organisation Code	
7. Author(s) Mohammad Ali Rezaizadeh and Shankar Mall				8. Performing Organisation Report No.	
9. Performing Organisation Name and Address University of Missouri Department of Engineering Mechanics Rolla, Missouri 65401-02449				10. Work Unit No.	
				11. Contract or Grant No. NAG1-425	
12. Sponsoring Agency Name and Address National Aeronautics and Space Administration Washington, DC 20546-0001				13. Type of Report and Period Covered Contractor Report	
				14. Sponsoring Agency Code 505-33-33-05	
15. Supplementary Notes  Langley technical monitor: Dr. W. S. Johnson This report is essentially M. A. Rezaizadeh's M.S. Thesis.					
16. Abstract A combined experimental-analytical investigation to characterize the cyclic failure mechanism of a simple composite-to-composite bonded joint was conducted. The cracked lap shear (CLS) specimens of graphite/epoxy adherend bonded with EC-3445 adhesive were tested under combined mode I and II loading. In all specimens tested, fatigue failure occurred in the form of cyclic debonding. The cyclic debond growth rates were measured. The finite element analysis was employed to compute the mode I, mode II, and total strain energy release rates (i.e., $G_I$ , $G_{II}$ , and $G_T$ ). A wide range of mixed-mode loading, i.e., $G_I/G_{II}$ ranging from 0.03 to 0.38, was obtained. The total strain energy release rate, $G_T$ , appeared to be the driving parameter for cyclic debonding in the tested composite bonded system.					
17. Key Words (Suggested by Author(s)) Adhesive joints, composites, cracked-lap-shear specimens, strain energy release rate, cyclic debonding, mixed-mode				18. Distribution Statement  Unclassified-Unlimited Subject Category 24	
19. Security Classif.(of this report) Unclassified		20. Security Classif.(of this page) Unclassified		21. No. of Pages 60	
				22. Price A04	

For sale by the National Technical Information Service, Springfield, Virginia 22161